Cretaceous Research 56 (2015) 691–701

Contents lists available at ScienceDirect

Cretaceous Research

journal homepage: www.elsevier.com/locate/CretRes

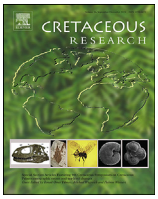

Orbitally forced sea-level changes in the upper Turonian–lower Coniacian of the Tethyan Himalaya, southern Tibet

Xi Chen [a, *], Chengshan Wang [a], Huaichun Wu [a], Wolfgang Kuhnt [b], Jianzhong Jia [c], Ann Holbourn [b], Laiming Zhang [a], Chao Ma [d]

[a] *State Key Laboratory of Biogeology and Environmental Geology, China University of Geosciences, Beijing 100083, China*
[b] *Institute of Geosciences, Christian-Albrechts-University, Kiel D-24118, Germany*
[c] *China National Offshore Oil Corporation, Beijing, 100010, China*
[d] *Department of Geoscience, University of Wisconsin-Madison, Madison, WI 53706, USA*

ARTICLE INFO

Article history:
Received 24 April 2014
Accepted in revised form 19 July 2014
Available online 16 September 2014

Keywords:
Late Turonian
Sea-level change
Tethyan Himalaya
Continental ice

ABSTRACT

Although the mid-Cretaceous is considered to be a typical interval of greenhouse climate and high sea level, cooling events associated with regressions were inferred in recent years. We conducted a biostratigraphic, chemostratigraphic, sequence stratigraphic and cyclostratigraphic investigation of upper Turonian–lower Coniacian marine strata in the Tethyan Himalaya zone, to retrace the sea-level variations and to clarify their global correlations. According to the planktonic foraminiferal zonation, the studied interval is part of the late Turonian–early Coniacian *Marginoruncana sigali* and *D. concavata* Zones. The carbon isotope curve shows a good correlation to reference curves in the Boreal and western Tethys realms with all major and minor late Turonian $\delta^{13}C$ events identified, indicating that the C-isotope curve provides an excellent tool for global stratigraphic correlation in the Turonian. Based on the lithological variations of clastic input and physical and chemical proxies, the succession is divided into two third order and eight fourth order sequences. Spectral analysis indicates that fourth order sea-level changes were linked to the astronomically stable 405-kyr eccentricity cycle. Comparison with classic global sea-level curves, we suggest that late Turonian–early Coniacian sea-level changes along the southeastern Tethyan margin were controlled by eustasy. The significant regressions during ~90–89.8 Ma and ~92–91.4 Ma, which are recorded in different continents, may be interpreted as the result of continental ice expansion, giving some support to the notion that ephemeral polar ice sheets existed even in the super-greenhouse world.

1. Introduction

The mid-Cretaceous, especially the Cenomanian-Turonian interval, is considered to be a typical interval of greenhouse climate with high sea-surface temperatures (SSTs) (Huber et al., 2002; Wilson et al., 2002; Bice et al., 2006; Forster et al., 2007a,b), high sea level as well as a much flatter equator-to-pole thermal gradient than today (Barron, 1983; Huber et al., 1995). Mid-Cretaceous upper ocean temperature estimates from oxygen stable isotope ($\delta^{18}O$) analyses of planktonic foraminifera typically indicate SSTs that are 8–20 °C warmer than modern values (Bice and Norris, 2002). In the Turonian-Coniacian interval, the mean annual temperature was over 14 °C (Tarduno et al., 1998). In addition $\delta^{18}O$ values indicate upper ocean waters as warm as ~30 °C at ~60°S paleolatitude in the late Turonian (Bice et al., 2003). Previous publications also suggested that average SSTs were ~10 °C higher during the Turonian than today (Huber et al., 1995; Wilson et al., 2002). These extremely high temperatures were probably linked to CO_2 concentrations 4–10 times higher than the pre-industrial level (Berner, 1994; Berner and Kothovala, 2001).

The sea level during this interval was estimated as tens of meters (Sahagian et al., 1996; Miller et al., 2003, 2004, 2005a,b) to more than 100 m (Haq et al., 1987; Haq, 2014) higher than the present day. Despite the generally high temperature and sea level in the Turonian, some short intervals of cooling (Bornemann et al., 2008; Forster et al., 2007a) and rapid sea-level changes were inferred, which may have been related to cyclic polar glacier growth and decay during intervals of reduced insolation in southern hemisphere high latitudes (Miller et al., 2004, 2005a, b). Although it is widely accepted that the warm Mesozoic climate was

---

* Corresponding author.
E-mail address: xichen@cugb.edu.cn (X. Chen).

http://dx.doi.org/10.1016/j.cretres.2014.07.010

undoubtedly punctuated by cooling events (Price, 1999; Price and Hart, 2002), it has been intensely debated whether these were sufficient to lead to the formation of polar ice (e.g. Barron, 1983; Kemper, 1987; Crowley and North, 1991; Frakes et al., 1992; Frakes and Krassay, 1992; Hallam, 1993; Chumakov, 1995; Bennett et al., 1996; Frakes, 1999; Oyarzun et al., 1999; Moriya et al., 2007; Ando et al., 2009).

In order to test the hypothesis of Cretaceous glacial-eustasy, we need to evaluate whether regional sea-level changes are globally coeval. The Cretaceous marine sequences, which are well exposed in the Tethyan Himalaya zone of southern Tibet, provide a unique opportunity to investigate the sea level record of the eastern Tethyan realm. We re-examined the planktonic foraminiferal biostratigraphy in the late Turonian–early Coniacian record of the Gongzha section in southern Tibet (Li et al., 2006) to determine the biozonal boundaries. Based on the biozones, the carbon isotope curve is correlated to the reference curve of Europe (Jarvis et al., 2006) to identify the major and minor isotopic events in the eastern Tethyan realm. In addition, we studied the lithology as well as chemical and physical proxies to establish relative sea-level fluctuations in the Tethyan Himalaya. Previous work showed that $\delta^{13}C$, $CaCO_3$, Mn, MS (magnetic susceptibility) and GR (gamma ray logging) were helpful proxies to study the effect of sea-level changes in marl/limestone alternation successions (e.g. Wendler et al., 2013; Boulila et al., 2008; Jarvis et al., 2001; de Rafélis et al., 2001; Miller et al., 2004). In this study we used $\delta^{13}C$, $CaCO_3$ and GR profiles as well as lithological descriptions to reconstruct a sea-level curve for the late Turonian–early Coniacian interval in the Tethyan Himalaya. Spectral analysis was used to detect orbital scale sea-level changes and to determine the age and duration of sea-level cycles. Finally, we correlated the regional sea-level changes to previously established sea-level curves to identify global signals and to assess possible mechanisms of sea-level change in the late Turonian-early Coniacian greenhouse world.

2. Geological settings

Cretaceous marine deposits in southern Tibet are mainly exposed in the Tethyan Himalaya tectonic zone (Fig. 1), located between the Higher Himalayan Crystalline Belts and the Indus-Yarlung Zangbo Suture Zone (Burchfiel et al., 1992). The Mesozoic strata in this area belong to two different tectonic domains: the passive continental margin of the Indian continental plate and the adjacent deep oceanic basin (Yu and Wang, 1990; Liu and Einsele, 1994). The Gyirong-Kangmar intracrustal thrust subdivides the Tethyan Himalayas into the northern and southern subzones of different lithological compositions (Liu and Einsele, 1994). During the mid-Cretaceous, the area was at a latitude of 21°S (Patzelt et al., 1996) and surrounded by an ocean connected eastward to the Pacific Ocean and westward to the Mediterranean Tethys (e.g. Scotese, 1991).

The studied area is located in the southern Tethyan Himalaya subzone, which formed the north margin of the Indian continent after it finally separated from Eastern Gondwana in the Early Cretaceous (Hu et al., 2010). During the mid-Cretaceous (late Albian–Santonian), the Tethyan Himalaya tectonic zone as passive margin drifted northward with the Indian continent (Garzanti and Hu, 2014). The studied section at Gongzha is situated ~50 km west of the city of Tingri on the north slope of the Zhepure Mountain (Li et al., 2006). The Cretaceous strata mainly consist of marly limestone couplets with a few limestones and calcareous shales. The positive carbon isotope excursion event at the Cenomanian-Turonian boundary (OAE2) is well developed in the section, although it is characterized by thin to medium bedded limestones instead of black shales as in other marine Cretaceous successions (Li et al., 2006). The Cenomanian-Turonian boundary is at 62 m in the section according to planktonic foraminifers and the end of the positive $\delta^{13}C$ excursion. The top of Turonian was placed at 88 m in the section by Li et al. (2006), whereas Wendler et al. (2009) argued that the Turonian-Coniacian boundary might be at ~137 m by correlating the $\delta^{13}C$ curve with the neighboring Zhepure section (Willems and Zhang, 1993), which is named Tingri section by Wendler et al. (2009), and the Eastbourne section of southern England (Jarvis et al., 2006). In the Gongzha section, the lower Turonian is characterized by thin to medium bedded calcareous wackestone layers that form a relief peak. From 85 to 90 m, the lithology is composed of marls or calcareous shales with thin bedded wackestone layers. From 90 to 145 m, it mainly consists of marl and marly limestone couplets except for two intervals of ~5 m thick thin bedded limestones (8–10 cm thickness for each single layer). The couplets are commonly a few cm to 20 cm in thickness. In a single couplet, the marl and limestone layers do not exhibit sharp contacts.

3. Materials and methods

We undertook detailed sedimentary logging, sequence stratigraphic analysis, geochemical sampling and Gamma Ray (GR) measurements in the upper Turonian–lower Coniacian part of the Gongzha section. High resolution (10–15 cm) GR data sets were directly measured at the outcrop face with a portable natural radioisotope analyzer CIT-2000F (Xinxianda co. ltd., China) with a detector of 5*5 cm square. Counts per seconds (cps) in selected energy windows were directly converted to concentrations of potassium, K (%), uranium, U (ppm) and thorium, Th (ppm). A 180 s time interval was applied at each measuring point with a vertical sampling step of 10–15 cm. In total 600 measurements were collected from the studied succession.

Thirty one samples from marls were selected between 85 and 142 m for micropaleontological analysis. About 100 g from each sample were submerged in water for several days and sieved over a 63 μm sieve. Generally, 10–20 g of sediment residue were initially examined for foraminifers and then treated with anionic tensides (REWOQUAT), which helped to completely break down the sample. In most cases tens to hundreds of moderate to well preserved planktonic foraminifers were obtained in the 63 μm to 1 mm size fraction of each sample. The planktonic foraminifers were identified under a binocular microscope and typical specimens were documented using a scanning electronic microscope. Approximately 20 thin sections of limestones or marly limestones were examined to determine the microfacies and lithologic changes of the interval.

Six hundred samples were collected for carbonate analysis from the 80–142 m interval in the section. The carbonate contents were estimated by using a carbonate bomb. About 0.3 g of dried sample were was ground to powder and dissolved in 5 ml hydrochloric acid of 10% concentration. According to the volume of CO_2, we can calculate the weight percentage of carbonate in the samples. Every 1 h, the same process was carried on 0.3 g pure $CaCO_3$ powder to estimate the temperature and pressure changes effect on the volume of CO_2.

In order to evaluate the cycle characteristics of the studied section, a multitaper method (MTM) of spectral analysis (Thomson, 1982) was conducted on the carbonate content and gamma ray data. The cycle length ratio method (Weedon, 2003) is applied to investigate the links between detected sedimentary cycles and the theoretical astronomical parameters. MTM power spectra analysis was performed using the SSA-MTM toolkit (Ghil et al., 2002). Robust estimates of background red noise with confidence limits at the 90%, 95% and 99% level were determined following Mann and